Garwan

PROGRAMME AND ABSTRACTS

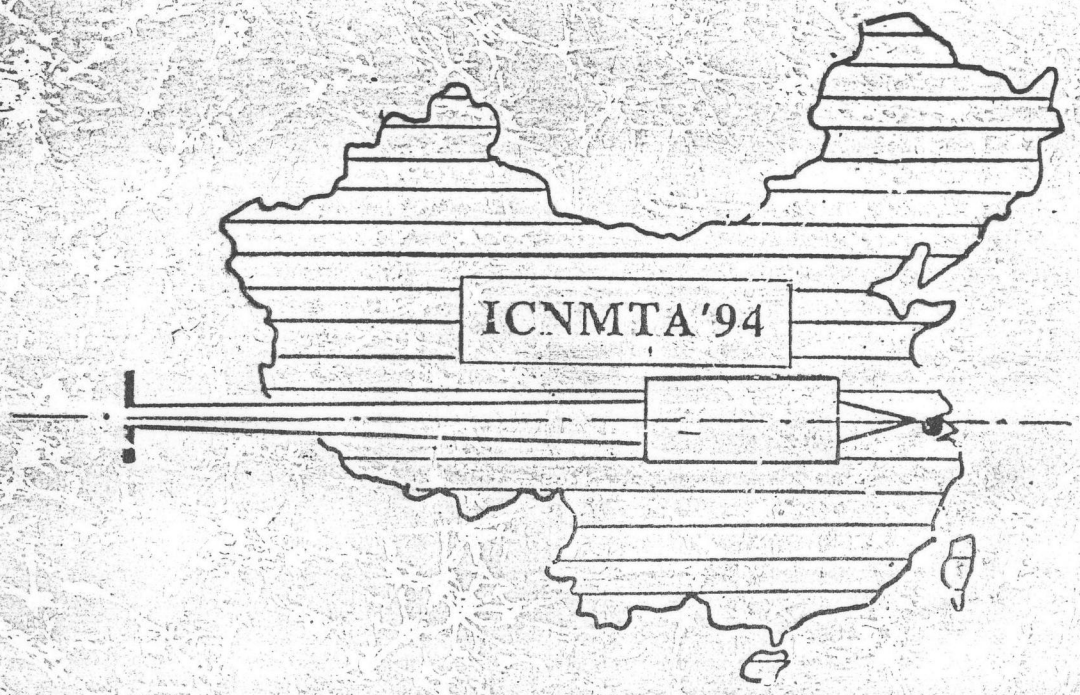

4TH INTERNATIONAL CONFERENCE ON NUCLEAR MICROPROBE TECHNOLOGY AND APPLICATIONS

Shanghai Institute of Nuclear Research, Academia Sinica,
And Fudan University
SHANGHAI, CHINA, 10–14 OCTOBER, 1994

purposes. Currents of the order of tens of pA can be maintained for the smallest beam spot sizes. The facility is now routinely applied in applications in the fields of geology, archeology, biology and materials technology.

The data-acquisition and analysis systems are based on a VAX/VMS computer system, a PC controlled scan system, the XSYS data acquisition system, the GeoPIXE suite of X-ray analysis software and the RUMP software package for RBS analysis. A VAX-station has recently been obtained to facilitate the use of various windows on one terminal, both for acquisition and analysis. The Dynamic Analysis method of obtaining quantitative elemental maps was recently installed and will be comprehensively reported on this conference. Detection systems include X-ray detection, an annular silicon surface barrier (SSB) detector at 176^0 for mainly RBS, a SSB detector at 30^0 for ERD and STIM and a secondary electron detector (channeltron).

The accuracy and precision of the PIXE system have been measured and found to be well within expected levels. Detection limits have been relatively low since the acquisition of a large area X-ray detector.

Features such as stepper motor controlled sample movement, active and passive beam stability control and planned on-demand beam pulsing will be discussed, establishing the NAC nuclear microprobe as a fully characterised tool for use in all mentioned fields of application.

Experience With the KFUPM Scanning Microbeam

T1 Oral 6

J. Nickel, M. Ahmed, and M. Garwan
Energy Resources Division, Research Institute, King Fahd University of Petroleum & Minerals, Box 1906, Dhahran 31261, Saudi Arabia

The scanning microbeam facility at King Fahd University of Pertroleum & Minerals (KFUPM), Saudi Arabia can focus a 2.5 MeV proton beam from the tandetron accelerator to a minimum spot size of 4μm x 4μm at a current of 100 pA, with a maximum scanning area of 540μm x 540μm. A micro-PIXE set up for elemental analysis and a Channeltron secondary electron detector for positioning the microbeam spot on the target are available. The data acquisition system, based on CERN's VALET-Plus software, permits collection and live display of the PIXE energy spectrum and multiple elemental distribution maps in color simultaneously.

Within the past year, several experiments have been performed to demonstrate the capabilities of the microbeam system. Analysis of a single pellet, about 1 mm in diameter, of a failed oil refinery catalyst showed non-uniform distribution of Fe over the scanned surface. Scanning of individual particles, 60-300μm in sizes, of powdered silica-based nickel catalysts revealed enrichment of Ni on the surface of the silica particles due to calcination process. Measurements of Cu and Fe distributions at the interface of a copper-steel friction weldment showed penetration of Cu into the steel region upto about 100μm. In wear studies of tungsten-carbide metal cutting tools, the tip of a spent tool which was used to machine a stainless steel work piece was found to have depositions of Fe and Mn from the work piece. The distribution maps of these two elements were not found to be correlated.

High-Intensity Submicron Microprobe Using a Single-Ended Accelerator with Very High Voltage Stability

T1 Oral 7

T.Kamiya, T.Suda and R.Tanaka
Takasaki Ion Accelerators for Advanced Radiation Applications,Japan Atomic Energy Research Institute, Takasaki, Gunma, 370-12 Japan

A new high-energy microbeam apparatus was constructed on a beam line of the JAERI 3 MV single-ended electrostatic accelerator in TIARA. In this apparatus, we are aiming to form high intensity submicron helium or proton beams, with the spot size at the target of less than 0.5 μm and with the beam current of more than 100 pA. High resolution micro-RBS or PIXE, and other new ion beam techniques will be available by utilizing these probes. The accelerator which can generate terminal voltage with the stability of within $\pm 1 \times 10^{-5}$, and the beam transport system which has a high energy-resolution beam analyzing section were provided in order to decrease the effects of chromatic

Experience with the KFUPM Scanning Microprobe

J. Nickel, M. Ahmed, A. Coban, M. Garwan

Energy Research Laboratory, Research Institute
King Fahd University of Petroleum & Minerals
Dhahran 31261, Saudi Arabia

Abstract

A scanning nuclear microprobe facility was installed at King Fahd University of Petroleum & Minerals (KFUPM), Dhahran, Saudi Arabia in late 1992. The analytical setup available on the microprobe includes PIXE, RBS and NRA. This paper gives an overview of the capabilities of the microprobe system by outlining some representative studies performed so far.

1. Introduction

The scanning nuclear microprobe facility at the Energy Resources Division of King Fahd University of Petroleum & Minerals, Dhahran, Saudi Arabia went into operation just over a year ago [1]. Built around a 3 MV tandetron accelerator, this microprobe has a minimum spot size of 4 x 4 μm^2 at a beam current of 50 pA, and a maximum scanning area of 540 x 540 μm^2. The target chamber is equipped with a Si(Li)-Detector for PIXE, a Surface Barrier Detector for RBS and a Sodium Iodide Detector for NRA mode of operation. A Secondary Electron Detector is used for viewing and positioning the sample. The data aquisition system developed here [2], based on CERN's 'VALET-Plus' software, permits collection and live display of one energy spectra at a time and up to twenty two-dimensional distribution maps simultaneously, each 64 x 64 pixels in size. Within the past year we tackeled a variety of problems, mainly in catalyst research and material science [3-8]. This paper gives brief descriptions of these experiments to demonstrate the capabilities of the microprobe system.

2. Measurements

2.1 Surface Agglomeration in a Spent Catalyst Pellet

Knowledge of the elemental distributions in catalysts is important in understanding their mechanism of operation, reason for failure and poisoning as well as in the reactivation of partially spent catalysts [3]. A used catalyst (2 mm in diameter) from a petroleum refinery was

investigated for the distribution of Pt, Rh and Fe over the surface. It was suspected by the supplier that the failure of this batch of catalysts was due to agglomeration of the catalytic elements Pt and Rh. Using μ-PIXE, we measured elemental distribution maps of the three elements from an area of 430 x 330 μm^2 on the sample surface of one pellet. The maps with a spatial resolution of about 5 μm show uniform distribution in Pt and Rh, whereas there is a markedly nonuniform distribution for Fe as shown in Figure 1. Fe probably appears as contamination during the catalytic process and selectively moves itself to better binding sites in the body of the catalyst [1].

2.2 Nickel Distribution in Silica-based Catalyst Grains

Supported Ni catalysts have applications in hydrogenation, stabilization and hydro-treating processes [4]. In order to better control their activity and selectivity, some studies have been aimed at their characterization. As very little is yet known regarding the location and behaviour of nickel particles on the support, we used the μ-PIXE technique to investigate the distribution of Ni across silica-based catalyst grains, 60-300 μm in size [5]. For this study the grains were embedded in epoxy resin and the surface polished to expose a layer from center to surface to the proton beam. Four samples with 1% and 5% Ni concentrations, both uncalcined and calcined, were analysed over an area of 540 x 540 μm^2 each. Ni was found to agglomerate in the uncalcined samples, specially those with the higher Ni concentration (Figure 2). In addition we observed a surface enrichment of Ni in the calcined sample with 5% Ni, campared with the uncalcined one,

indicating migration of Ni from the interior of the grain to the surface due to the effect of calcination process.

2.3 Iron Distribution in a Friction Weld Interface

In the friction welding process, the joining surfaces of the samples are heated to desirable temperature through frictional heat and then a forging pressure is introduced to weld the parts. One of the applications of the friction welding process is in joining dissimilar metals as copper and steel. To obtain sound welds and determine the limits of the welding conditions, analysis of heat transfer mechanism taking place during the welding process becomes necessary.
We could show by μ-PIXE analysis of the Fe distribution within the friction weld interface (Figure 3), that the maximum heat affected zone is far from the center and close to the surface where the temperature gets its highest and therefore melting would possibly occur in this region [6].

2.4 Wear Studies of Tungsten Carbide Cutting Tools

Bringing a useful life of a cutting tool to an end is the gradual or progressive wearing away of certain regions of the rake face and flank face of the cutting tool. Three forms of wear are known to occur: adhesion, abraison and diffusion wear. These processes, which occur at the interface between tool, chip and work piece, involve the movement of atoms between the materials by diffusion and the loss of tool material to the chip or work piece by adhesion or abraison. The extent

of tool wear is a function of the cutting conditions and the properties of the work piece and cutting tool materials. Conventional tool wear studies are not explicitly capable of identifying the wear mechanisms acting on the tool and the conditions under which they occur.
Using the μ-PIXE technique, we analysed the rake face and flank face of a worn sample of uncoated WC(Co) tool insert used in machining 'BSEN1A' steel. Elemental distribution maps of the major constituents of the work piece (Mn, Fe) and the tool insert (W) on the rake face and primary flank face of the used tool were constructed from the data. Figure 4 shows as an example the distribution of Mn and Fe across the rake face of a tool insert. The main outcome is the difference in the distributions of these two elements although both of them originate from the work piece. The distribution of Fe appears to reflect the adhesion of the chip to the tool whereas the distribution of Mn appears to show the presence of temperature dependant diffusion wear mechanism [7].

2.5 Nitrogen Depth Profile of Plasma-nitrited Steel

Plasma nitriding and coating processes are techniques to optimize surface properties such as hardness and wear resistance. Detecting the outcoming γ-rays from the $^{15}N(p, \alpha\gamma)^{12}C$ reaction at the 1649 keV resonance energy, we studied the nitrogen distribution inside a plasma-nitrited 'EN40B' steel sample using a beam spot size of about 20 x 20 μm^2 [8]. The thickness of the nitrogen layer was determined to 120 ± 10 μm. The sample surface was localized by detecting iron X-rays from the same sample region using μ-PIXE. Due to the low cross sections of nuclear reactions the present measurement has only poor statistics, so

that we could not determine the nitrogen profile below the layer. The nitrogen profile data in Figure 5 also still includes background counts mainly from the $^{19}F(p, \alpha\gamma)^{16}O$ reaction, explaining that in greater depths the data points doesn't come down to zero.

3. Conclusion

Looking at the variety of problems we tackeled so far, the μ-beam setup can contribute to the investigations of a wide spectrum of technical and engineering problems. With its strength in detecting distributions of trace elements it is at KFUPM probably also useful in investigating goeological phenomena like diffusion processes. Due to our limited spatial resolution we could not yet utilize the setup in marine biology and solid state physics.

Depth profiles measured with RBS and NRA, by means of a beam perpendicular to the surface, are limited in range to about 2 μm. For our μ–beam setup spatial resolution limits are 4 μm for PIXE and 20 μm for RBS and NRA (Table 1). Both methods cannot resolve the technical important range of 2-10 μm. This can be a motivation to investigate the present limits of our spatial resolution.

Acknowledgement

This work and the tandetron facility is fully supported by the Reseach Institute of King Fahd University of Petroleum & Minerals. We would like to thank Dr. J. Anabtawi, S. M. Pillai, Dr. A. Rahman, Dr. A. Shuaib and Dr. B. Yilbas.

References

[1] M. Ahmed, J. Nickel, A. B. Hallak, R. E. Abdel-Aal, A. Coban, H. A. Al-Juwair and M. A. Aldaous. Nuclear Instruments and Methods in Physics Research B82 (1993) 584-588.

[2] Y. Perrin, R. Bagnara, T. Berners-Lee, W. Carena, R. Divia, C. Parkman, J. Peterson, L. Tremblet and B. Wessels. Data Handling Division, CERN, Geneva, 1988.

[3] C. F. Scofield, L. B. Bridwell and C. J. Wright. Nucl. Inst. and Meth. 191 (1981) 379.

[4] G. Wendt et al, J. Chem. Soc., Faraday Trans. 1, 79, 2013 (1983).

[5] A. Rahman, M. H. Mohamed, M. Ahmed and J. Nickel. Accepted to Thirteenth International Conference on the Application of Accelerators in Research and Industry, University of North Texas, 7.-10. November 1994.

[6] A. Z. Sahin, B. S. Yilbas, M. Ahmed and J. Nickel. Submitted to Proceedings of the Institution of Mechanical Engineers, Part B, Journal of Engineering Manufacture, London, Great Britain.

[7] A. N. Shaib, J. Nickel and A. Ahmed. Accepted to International Conference of Nuclear Microprobe Technology and Applications 1994, Shanghai, China, from 10.-14. October 1994.

[8] J. Nickel, A. Coban, B. Yilbas, M. Ahmed, S. Sahin and M. Garwan. Accepted to International Conference of Nuclear Microprobe Technology and Applications 1994, Shanghai, China, from 10.-14. October 1994.

Captions for Figures

Figure 1 Surface distribution of Fe and Pt on a spent catalyst pellet. Darker shades on the grey scale indicates higher concentration.

Figure 2 Catalyst powder with 5% nickel. μ-PIXE measurements of Si and Ni distributions over individual silica particles. Darker shades on the grey scale indicates higher concentration. Picture size is 540 x 540 μm^2 each.

Figure 3 μ-PIXE measurement of Fe distribution within a friction weld interface.

Figute 4 Distributions of Mn and Fe across the rake face of an uncoated WC(Co) cutting tool tip. Darker shades on the grey scale indicates higher concentration.

Figure 5 N depth profile of a plasma nitrited steel sample.

Captions for Tables

Table 1 Experimental conditions for the μ-beam setup.

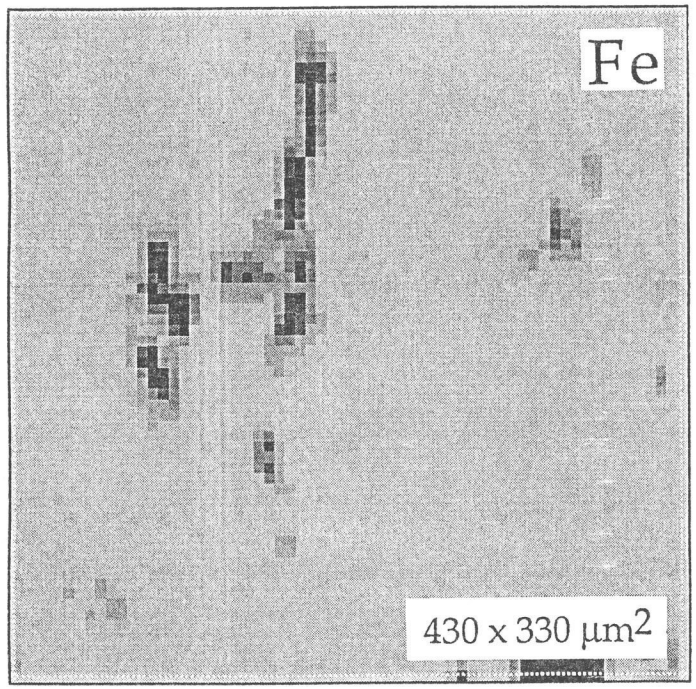
Fe
430 x 330 µm2

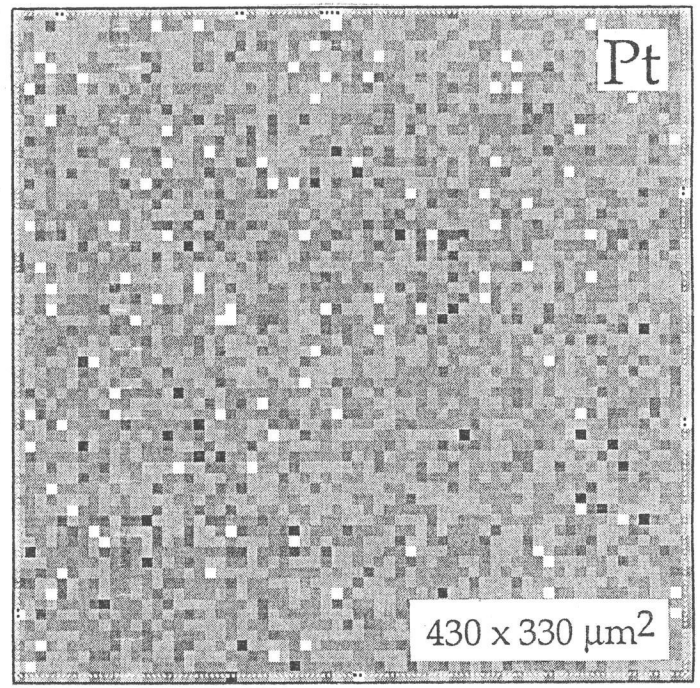
Pt
430 x 330 µm2

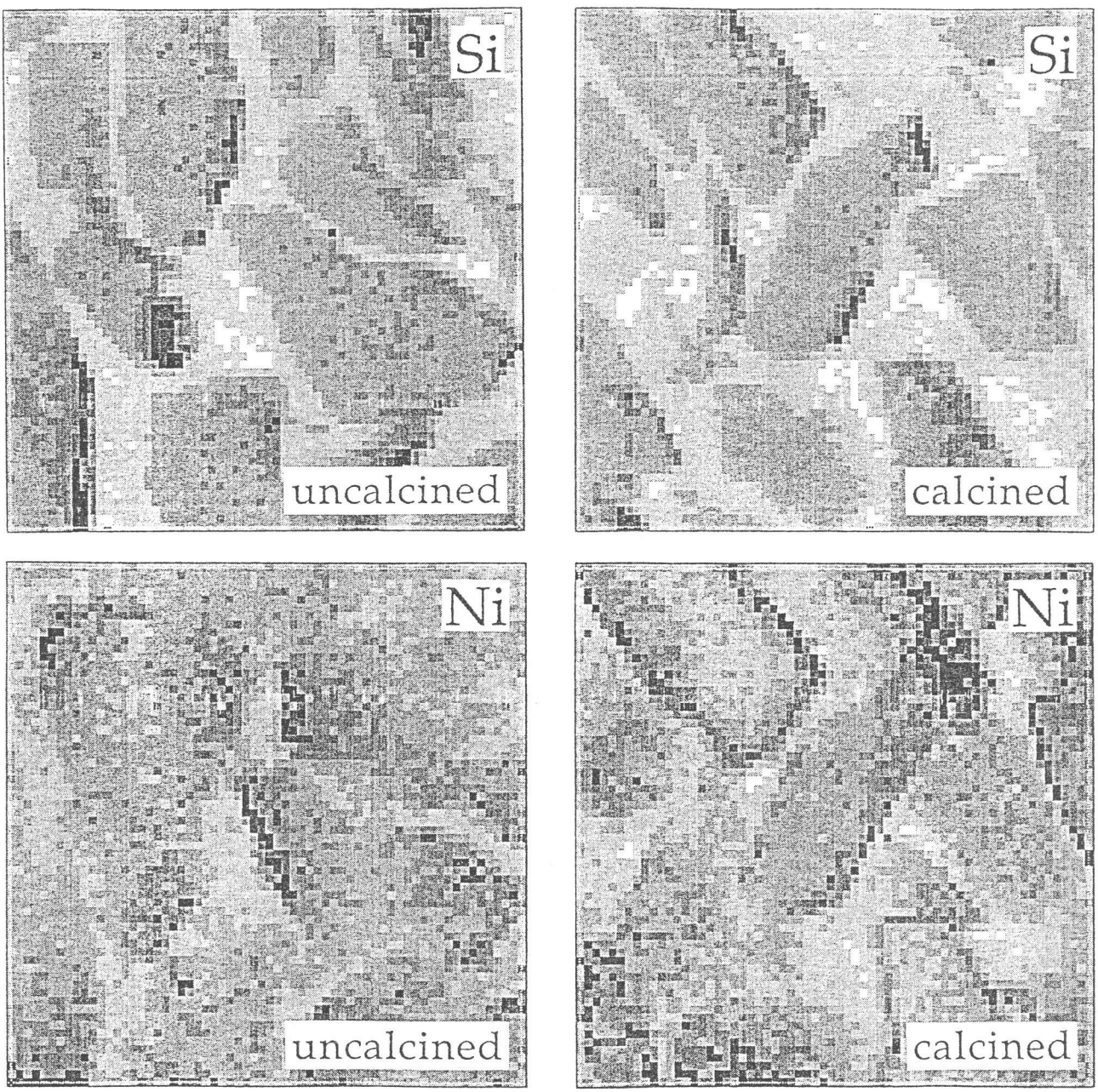
Si
uncalcined
Si
calcined
Ni
uncalcined
Ni
calcined

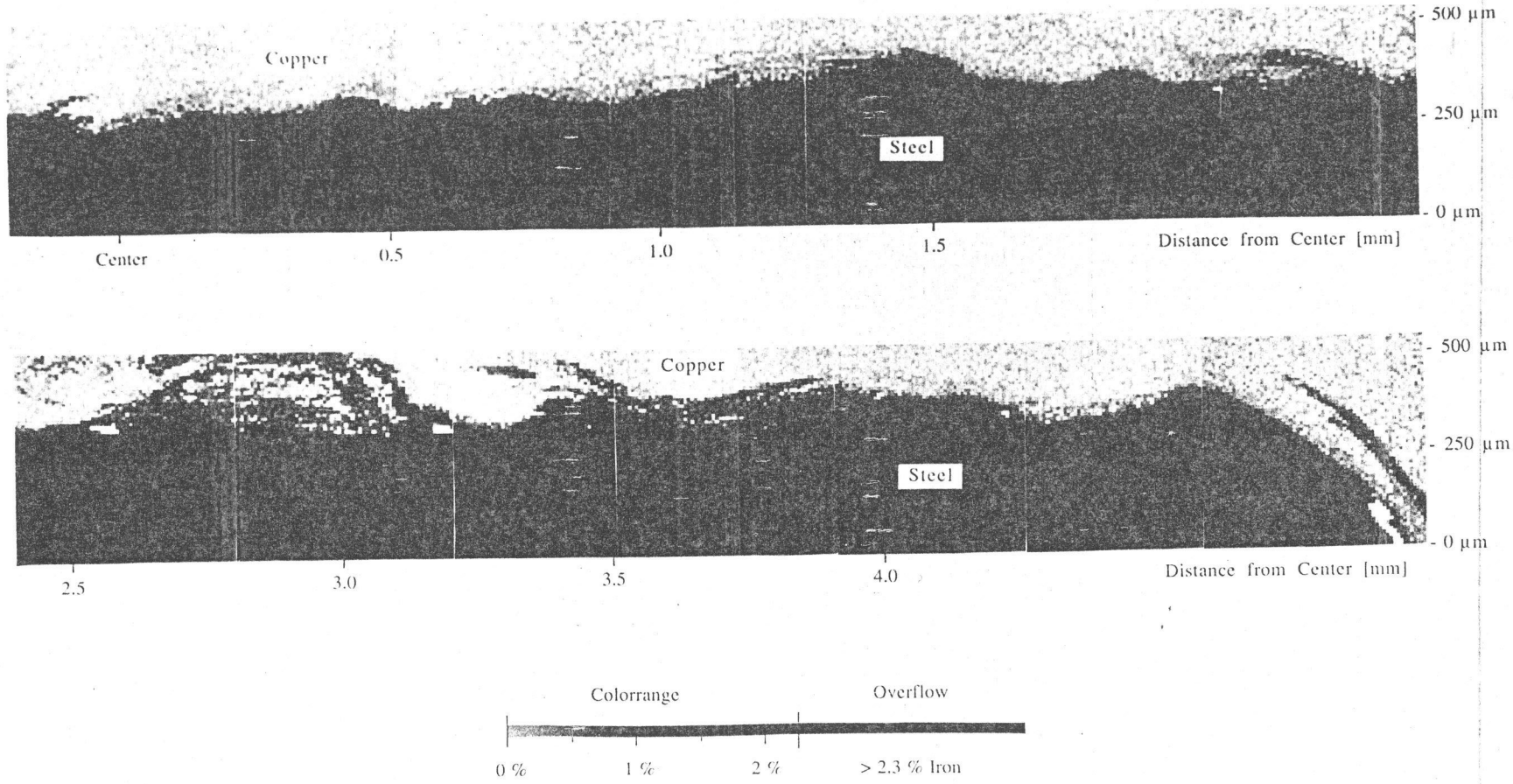
Copper
Steel
500 µm
250 µm
0 µm
Center
0.5
1.0
1.5
Distance from Center [mm]
Copper
Steel
500 µm
250 µm
0 µm
2.5
3.0
3.5
4.0
Distance from Center [mm]
Colorrange
Overflow
0 %
1 %
2 %
> 2.3 % Iron

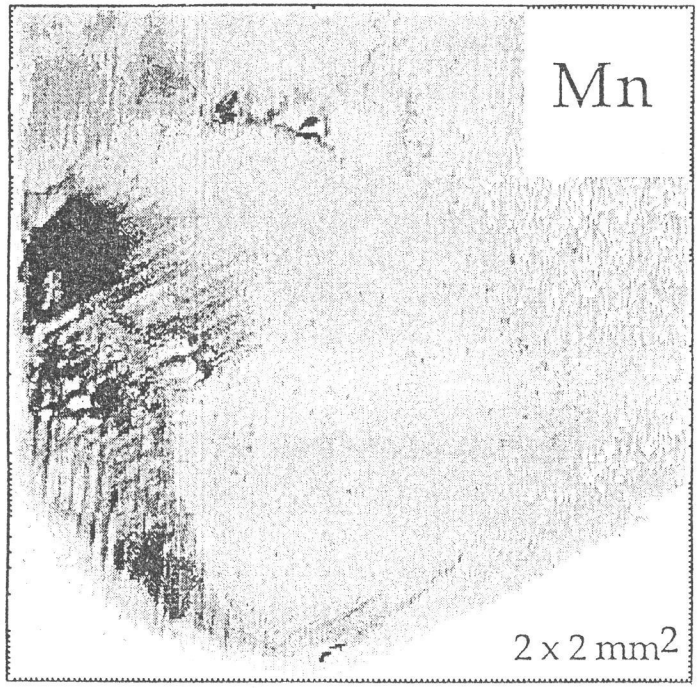
Mn
2 x 2 mm2

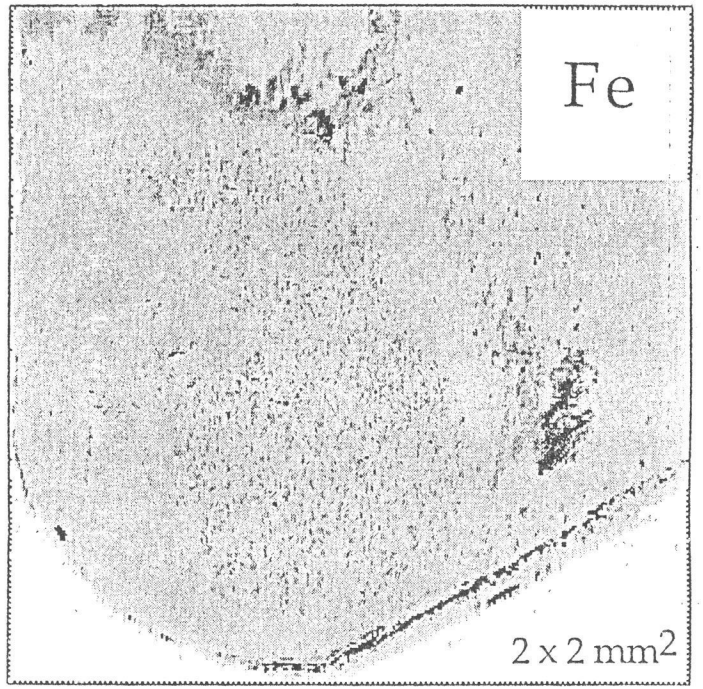
Fe
2 x 2 mm2

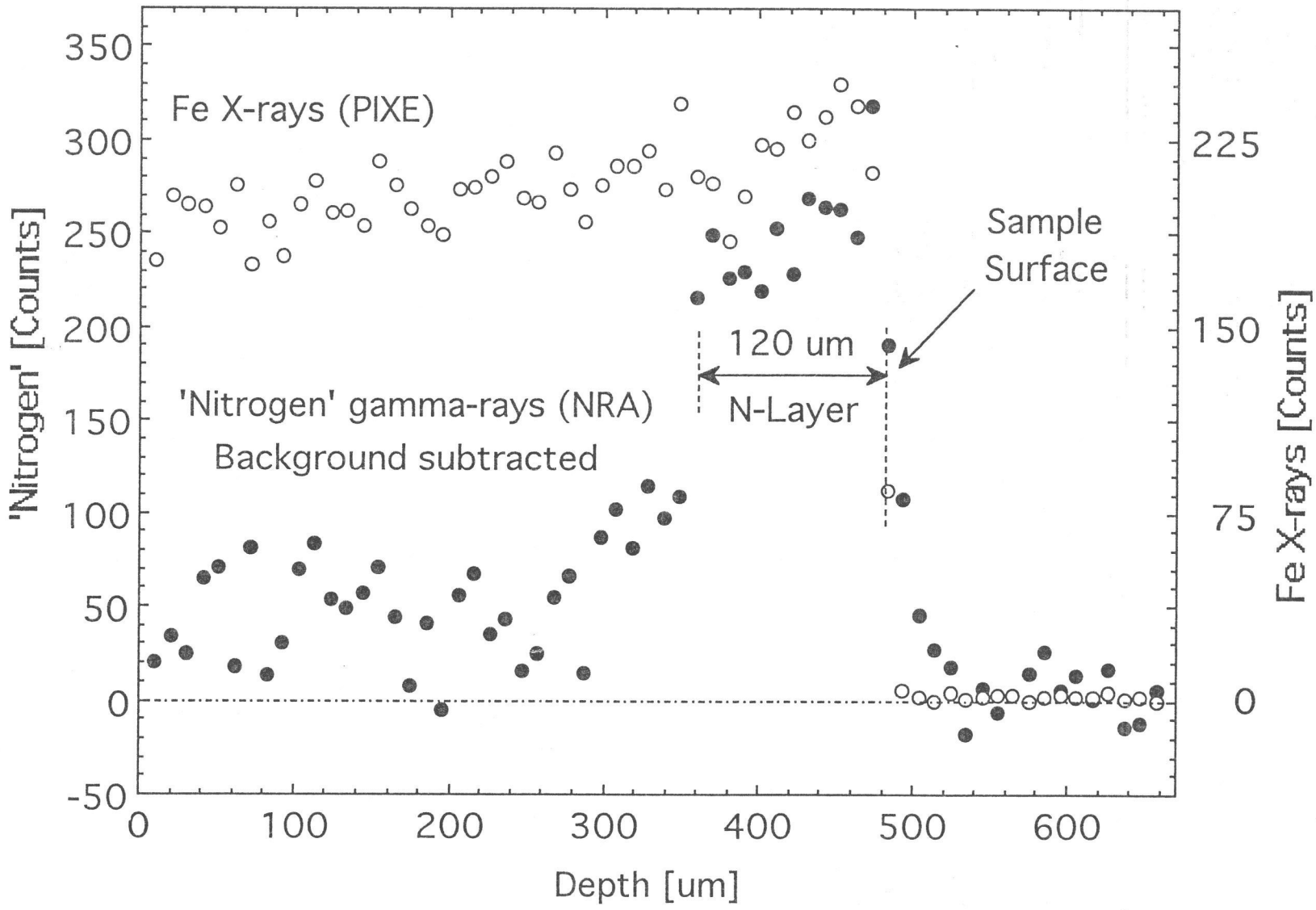
Fe X-rays (PIXE)
'Nitrogen' gamma-rays (NRA)
Background subtracted
120 um
N-Layer
Sample
Surface
'Nitrogen' [Counts]
Fe X-rays [Counts]
Depth [um]
350
300
250
200
150
100
50
0
-50
225
150
75
0
0
100
200
300
400
500
600

Beam	Energy	Current	Spot Size [um x um]	Brightness [pA / um^2 x mr^2]	Method
p^+	2.5 MeV	50 pA	~4 x 4	8	PIXE, Z<20
p^+	2.5 MeV	800 pA	~10 x 10	3	PIXE, Z>20
p^+	900 keV	80 nA	~20 x 20	0.9	NRA
α^{++}	2.5 MeV	4 pA	~10 x 10	0.02	for Comparison